ACS Sustainable Chemistry & Engineering

pubs.acs.org/journal/ascecg

Research Article

Recycling Plastic Waste by Solid Phase Mixing

Alina Vozniak,[‖] Ramin Hosseinnezhad,[‖] Artur Rozanski,[‖] Fahmi Zaïri,[‖] Iurii Vozniak,*[,‖] and Roman Kulagin*[,‖]

Cite This: *ACS Sustainable Chem. Eng.* 2025, 13, 1203−1212

Read Online

ACCESS | Metrics & More | Article Recommendations | Supporting Information

ABSTRACT: The global plastics problem poses significant environmental, energy, and climate challenges. Various innovative strategies have been proposed for recycling plastics, either in open or closed loops, each addressing different aspects of the problems hindering the achievement of a circular economy. Amidst these efforts, the reuse of mixed plastic waste still remains a particular challenge, arising from immiscibility, resulting in materials with suboptimal properties. In this context, we report a novel recycling strategy based on high-pressure solid-phase mixing of plastic wastes, ensuring the conversion of a binary immiscible polymer mixture into a mixture consisting entirely of the polymer−polymer interphase. The proposed recycling strategy represents a significant advancement as it allows for the production of mixtures with enhanced mechanical properties, all while avoiding the degradation of the initial molecular weight of the polymeric components. The demonstrated effectiveness spans a range of immiscible polymer pairs, including polyolefins, polystyrene, and polyesters, which collectively constitute about 70% of mixed plastic waste.

KEYWORDS: *recycling, plastic waste, homogeneous mixing, immiscible polymers, solid-phase mechanical recycling*

INTRODUCTION

The effective recycling of plastics continues to be a hot topic, essentially involving the development of innovative strategies for their sustainable reuse and waste reduction.[1] Although mechanical recycling is currently still the most widely used strategy for plastics recycling,[2−5] a new strategy is increasingly being explored—the depolymerization of chemically recyclable polymers into their starting monomers.[6−9] This strategy is characterized by a closed recycling loop, which is welcomed in the circular polymer economy. A key challenge is to design chemical bonds in chemically recyclable polymers to allow effective bonding and reversible cleavage. Driven by this challenge, a number of innovative approaches have recently been developed that enable highly efficient and reversible reactions, while maintaining a low energetic barrier to bond cleavage and high recovery rate of monomers (greater than 95%).[10−13] A number of polymers have been successfully tested: polyethylenes,[14] polyesters,[15,16] polycarbonates,[17] poly(cyclopentencarbonate),[18−20] polyimine,[21] and cross-linked supramolecular polyureas.[22] At this juncture, only single-phase systems can be considered for recycling by depolymerization, albeit these include such inert polymers as polyethylene, polypropylene, and polystyrene. However, lowering to the monomer level is not always economically justified and, in some cases, can be associated with major difficulties. In particular, depolymerization of mixed plastic waste can be associated with the risk of side reactions, leading to mixed products that cannot be recovered as monomers. Among the significant contributions to the field is the solid-state shear pulverization (S3P) technique, which is established for the in situ compatibilization of two or more incompatible polymers.[23−27] This technique advances plastic recycling by the wet-mechanical processing of mixed waste fractions. It effectively bridges the gap between traditional dry processing of mixed plastic waste and chemical plastic recycling via thermo-chemical conversion. Additionally, S3P offers a valuable solution to the challenges posed by immiscible polymers in waste plastics during the recycling process.

Mixed plastics comprise the majority of plastic waste. Estimates suggest that if mixed plastic waste could be effectively recycled, the value of the products recovered would exceed US$250 billion per year.[28] Further, entirely new strategies could be built around the recycling of mixed plastic waste. However, the difficulty of mixing immiscible macromolecules is a canonical problem that limits the performance of the polymer blends produced from them. This comes from very low entropy of mixing, which is about 1/N less than that of mixing the N monomers that make it up. However, there are specific features that distinguish macromolecular systems from those studied in classical colloid chemistry. These include the formation of an interphase, or intermediate layer, between the mixed components which is

Received: June 3, 2024
Revised: October 22, 2024
Accepted: October 23, 2024
Published: January 12, 2025

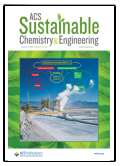

due to the effect of a number of thermodynamic and kinetic factors.[29] In particular, this interphase layer is the region where even immiscible macromolecules mix. Nevertheless, the amount of interphase in immiscible macromolecular systems is small and has no effect on changing the degree of miscibility. In many respects, however, it is the interphase that determines the physical and mechanical properties of polymer blends.

Although there are some methods for homogeneous mixing of immiscible macromolecules based on the use of supramolecular complexation, porous coordination polymers, and fluid interfaces,[30−33] they are nevertheless quite sophisticated and their use in recycling may have some technical limitations. Compatibilization of immiscible mixed-plastic chains is also possible. In particular, new compatibilization strategies have recently been presented in which dynamic cross-linkers are installed in situ in immiscible mixed plastics[34] or physical alloying is used in which a transient pressure is applied cyclically.[35−38] Here, however, it is necessary to distinguish between the advantages of miscibility and compatibilization. Miscibility involves the formation of a homogeneous single phase at the molecular level, which allows the properties of the resulting blends to be infinitely adjusted depending on the nature and content of the components, while compatibilization guarantees the preservation of distinct phases interconnected by macromolecules that tie across interphases and can be useful when the components of the mixed plastics have unique properties that need to be preserved.

Here, we propose a new strategy for recycling mixed plastic waste, involving the formation of homogeneous blends through treatment in the solid phase by using high-pressure torsion (HPT). A proposed mechanism of homogenization of mixed plastic wastes is monotonic mechanical reduction of the polymer phases to nanosize during the accumulation of plastic deformation. In this case, a decrease in the size of polymer phases should be accompanied by an increase in the proportion of polymer−polymer interphase, and eventually, the difference between polymer phases and interphase should disappear. The role of high pressure is to ensure close contact between the polymer phases and codeformation of the polymer phases down to the nanometer scale, while avoiding localization of the deformation in one of the phases. This approach has been approved for mixing immiscible metal alloys.[39−43] We demonstrate the transition from immiscible to miscible at nanometer scale polymer blends under HPT conditions using the example of immiscible blends based on polyolefins, polystyrene, and polyesters. This choice is due to the fact that they represent about 70% of mixed plastic waste.[44]

METHODS

Materials. Acrylonitrile-butadiene-styrene copolymer (**ABS**; Terluran GP-22), having melt flow index, MFI = 18 g/10 min (220 °C/10 kg, ASTM D1238), poly(ethylene terephthalate) (PET; EKOPET 80BB) with MFI = 16 g/10 min (220 °C/2.16 kg, ASTM D1238), polylactide (**PLA**; Luminy L175) with MFI = 8 g/10 min (210 °C/10 kg, ASTM D1238), polybutylene terephthalate (**PBT**; Crastin 6129 NC010) with MFI = 8 g/10 min (250 °C/2.16 kg, ASTM D1238), glycol-modified polyethylene terephthalate (**PET**; Eastar Copolyester 6763) with MFI = 8 g/10 min (265 °C/2.16 kg, ASTM D1238), high density polyethylene (**HDPE**; Lupolen 5261Z) with MFI = 2.0 g/10 min (190 °C/2.16 kg, ASTM D1238), polypropylene (**PP**; Moplen HP500N) with MFI = 12.0 g/10 min (230 °C/2.16 kg, ASTM D1238), and polystyrene (**PS**; Synthos PS GP 585X) with MFI = 8.0 g/10 min (200 °C/5.0 kg, ASTM D1238) were used in the experiments.

An initial blend with 50 wt %/50 wt % polymer components was produced on the Flashforge Creator pro three-dimensional printer by alternately depositing layers of blended polymers. Angular displacement of the layers was 90°. Printing of two-layer blends required an additional technological layer to provide the die, leaving the printing zone when the material is alternated. The temperatures of the extruder were as follows: 240 °C/240 °C (ABS/PET), 220 °C/270 °C (PLA/PBT), 220 °C/240 °C (PLA/PET), 240 °C/270 °C (PET/PBT), and 250 °C/250 °C (HDPE/PS, PP/PS). The temperature of the support was: 110 °C (ABS), 60 °C (the rest of the materials). In all cases, the thickness of the melt layers was 0.2 mm. Recycled counterparts were obtained by several cycles of reprocessing the corresponding polymers in a single-screw extruder (PlastiCorder PLV 151, Brabender; D = 19.5 mm, L/D = 25, and 30 rpm, temperatures of the four zones: 180/190/200/210 °C) and subsequent molding with an injection machine (Battenfeld H45210, injection temperature was set to 210 °C, injection rate was 10 cm^3/s), the process of which is described in detail in refs 45−47. Melt blends were produced with a Brabender batch mixer (Duisburg, Germany) operating at 190 °C (HDPE/PS, PP/PS, rHDPE/rPS, rPP/rPS) and 260 °C (ABS/PET, PLA/PET, PET/PBT, and PLA/PBT) for 10 min at 100 rpm.

High-Pressure Torsion. The samples with initial diameter 15 mm and thickness 1.5 mm underwent deformation using an HPT machine (Figure 1) with a quasi-constrained anvil design; one anvil featured a

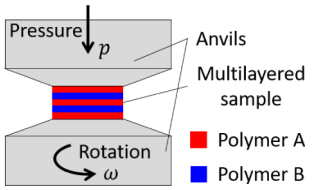

Figure 1. Schematic of high-pressure torsion (HPT).

0.3 mm groove, and the second was flat. The deformation involved 50 revolutions at a rotational speed of ω = 5 rpm. Polymers were placed between the anvils, and after reaching the required pressure level p = 1 GPa, torsional deformation occurred, and the selected pressure was consistently maintained by an automatic control system. Processing took place at ambient temperature, with a laser pyrometer monitoring the anvils' temperature near the sample. The number of revolutions of the anvil determines the amount of accumulated plastic shear strain, γ, according to the formula: $\gamma = 2\pi N \cdot r/h$, where r and h are the radius and thickness of a disk-shaped sample, respectively, and N is the number of rotations of the anvils.

Characterization Techniques. Solid-state NMR spectra were recorded on a Bruker AVANCE III WB 400 MHz spectrometer. The spinning rate for all experiments was 6 kHz. 13C cross-polarization magic-angle spinning spectra were obtained under two-pulse-phase-modulating proton decoupling. A recycle delay is 2 s. 1H spin−lattice relaxation time measurements both in the laboratory and in rotating frames T_1 and $T_{1\rho}$, respectively, were measured at room temperature by a saturation recovery method and a spin lock method, respectively.[48]

Thermal behavior of samples was probed with a DSC Q20 differential scanning calorimeter (TA Instruments) during heating with the rate of 10 °C/min. Samples of the 7−8 mg mass were cut out from initial and HPT-processed blends and crimped in standard Al pans. The DSC cell was purged with dry nitrogen during the measurements (50 mL/min). The DSC curves shown in Figure 2 correspond to the second heating scan. The first heating scan was used to remove residual stresses and erase any kinetic effects.

The TGA was performed from room temperature to 600 °C at 10 °C/min with a Rigaku Instrument Thermo plus TG 8120 in a nitrogen atmosphere.

The oxidation induction time (OIT) was measured with a DSC 910 differential scanning calorimeter (Du Pont Instrument). OIT was determined as the time (minutes) until the onset of oxidation during heating in an oxygen environment. The test temperature started at 20

https://doi.org/10.1021/acssuschemeng.4c04557
ACS Sustainable Chem. Eng. 2025, 13, 1203−1212

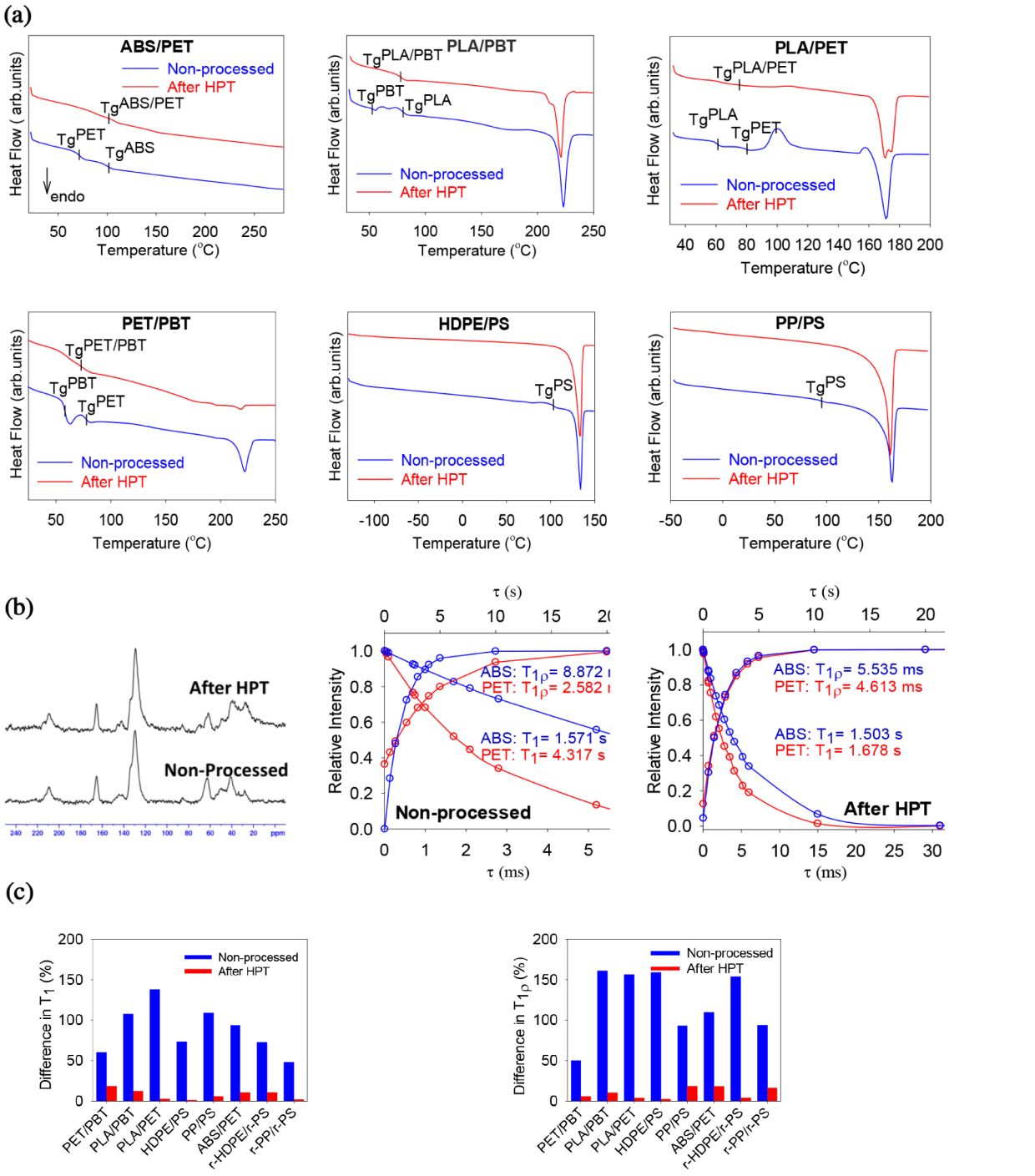

Figure 2. DSC thermograms of initial (nonprocessed) and HPT processed blends (a); ^{13}C CP/MAS NMR spectra and spin−lattice relaxation time measurements of ABS/PET initial and HPT processed blends to observe T_1 recovery and $T_{1\rho}$ decay curves for CH_2 of PET (red colored) and methyne carbon of ABS (blue colored) (b); difference of T_1 and $T_{1\rho}$ percentages before and after HPT for the all studied blends expressing the relative difference between the values as a percentage of their average (c). The observed behavior of the merging of T_1 recovery curves and $T_{1\rho}$ decay curves of the mixed phases ABS and PET is typical for other studied blends subjected to HPT. The corresponding T_1 and $T_{1\rho}$ data are listed in Table S1.

°C and increased with a heating ramp of 10 °C/min until an isothermal temperature was reached. The isothermal temperature was 210 °C.

The average molecular weights (M_n and M_w) were determined using a Gel Permeation Chromatography (GPC) system comprising (Agilent G1379A Degasser coupled to Agilent Pump 1100 Series), two PLGel 5 μMIXED-C columns, and two different laser photometers as detectors, namely, Wyatt Optilab Rex differential refractometer and Dawn Eos (Wyatt Technology Corporation, Santa Barbara, CA, USA). ASTRA 4.90.07 software (Wyatt Technology Corp.) was used for data collection and processing. The elution was carried out using dichloromethane at a flow rate of 0.8 mL min^{-1} at room temperature. The polydispersity index (PDI) was measured using the dRI signal, with the elution times calibrated with narrow-distribution polystyrene standards. The MALLS photometer allowed us to determine the absolute molecular weight directly from the angular dependence of the scattered light intensity.

https://doi.org/10.1021/acssuschemeng.4c04557
ACS Sustainable Chem. Eng. 2025, 13, 1203−1212

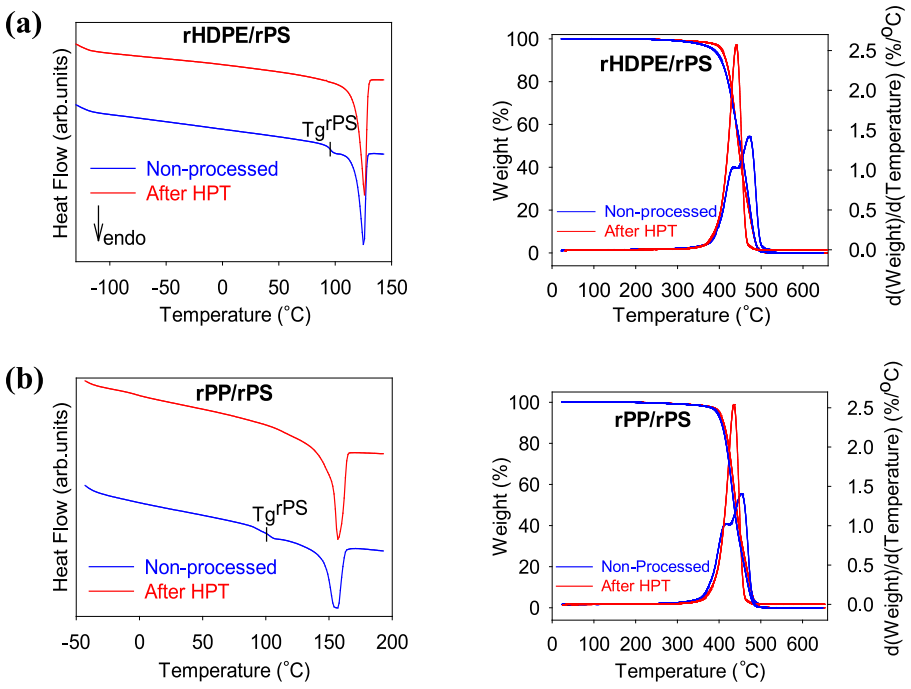

Figure 3. DSC and TGA thermograms of initial and HPT processed rHDPE/rPS (a) and rPP/rPS (b) blends. Data are for systems that have undergone 5 recycling cycles.

Transmission electron microscopy (TEM) was performed using a Tesla BS 500 electron microscope at 90 kV. Samples were prepared as thin sections approximately 60 nm thick using an ultramicrotome (PowerTome PC, Boeckeler, USA) equipped with a 35° diamond knife (Diatome, Switzerland). No staining or any other chemical treatment was applied to sections prior to observation.

Scanning electron microscopy (SEM) was performed by using a JSM-5500 LV scanning electron microscope from JEOL (Tokyo, Japan). Before examining the morphology of the cryogenic fractures with the JEOL JSM-5500 LV scanning electron microscope, PLA/PBT and PLA/PET were enzymatically etched for 1 week as described elsewhere.[49]

Microhardness H was determined with a micro-Vickers hardness tester. An indentation was made on the specimen by a diamond indenter through the application of a load p = 20 g. The size of the resultant indentation was measured with the help of a calibrated optical microscope, and the hardness was evaluated as the mean stress applied underneath the indenter. The uniformity of H distribution over the sample surface was estimated by value of dispersion D_H determined by the following formula:

$$D_H = \sqrt{\frac{1}{n(n-1)} \sum_{i=1}^{n} (\bar{H} - H_i)^2}$$

where n—number of measurements, H_i—result of an individual measurement of microhardness value, and $\bar{H}$—average microhardness value.

The mechanical properties of nonprocessed and HPT processed blends were evaluated using a tensile testing machine (Instron, Model 5582). The samples were cut into a rectangular shape measuring 15 × 5 mm with an initial distance of 10 mm between the clamps. The crosshead speed was set at 5%/min, and the sample under each condition was tested five times. Yield strength and modulus of elasticity were calculated based on the stress−strain curve of each sample. Due to the small size of the HPT-treated specimens, it was not possible to evaluate the strain at break of the blends as the lack of an oar-shaped specimen resulted in stress concentration at the locations where the specimens were clamped in the grips, leading to their premature failure.

RESULTS

Evaluation of High-Pressure Solid Phase Mixing. The term miscibility is used to describe a blend containing two or more components that are capable of forming a single-phase system that is homogeneous down to the nanometer or even molecular level.[50] Thermodynamics provides a clear way to predict whether a binary blend is miscible or immiscible and allows a quantitative determination of polymer−polymer interaction energies. While the above definition of miscibility is unambiguous, as it corresponds to a precise thermodynamic description of the system, the experimental determination of polymer blend miscibility is not free of ambiguities in practice. This is because the experimental determination of homogeneity in a blend is dependent on the experimental probe, and a system that appears to be single-phase if examined at sufficiently large length scales may not be truly miscible at the nanometer or molecular level.

To evaluate the length scale of homogeneity in polymer blends, DSC, TGA, and 1H spin−lattice relaxation time measurements both in the laboratory and in rotating frames (T_1, $T_{1\rho}$) using 13C cross-polarization magic-angle spinning NMR experiments were chosen. DSC and TGA are used to verify homogeneity at the micro level, and solid-state NMR at the nano level. It is known that each component of the blend is characterized by its own glass transition temperature T_g, decomposition temperature T_d, and spin−lattice relaxation time. With improved miscibility, both the glass transition temperatures and the individual decomposition stages of the mixed phases should move toward each other (according to the rule of mixtures). The spin−lattice relaxation times for each of the polymer phases should also tend to converge. For a miscible polymer blend, both the glass transition temperatures and the decomposition temperatures should converge to a single value as the miscible blend should glaze and decompose uniformly. Additionally, the relaxation times for both polymers should be the same as 1H spin diffusion occurs between all

https://doi.org/10.1021/acssuschemeng.4c04557
ACS Sustainable Chem. Eng. 2025, 13, 1203−1212

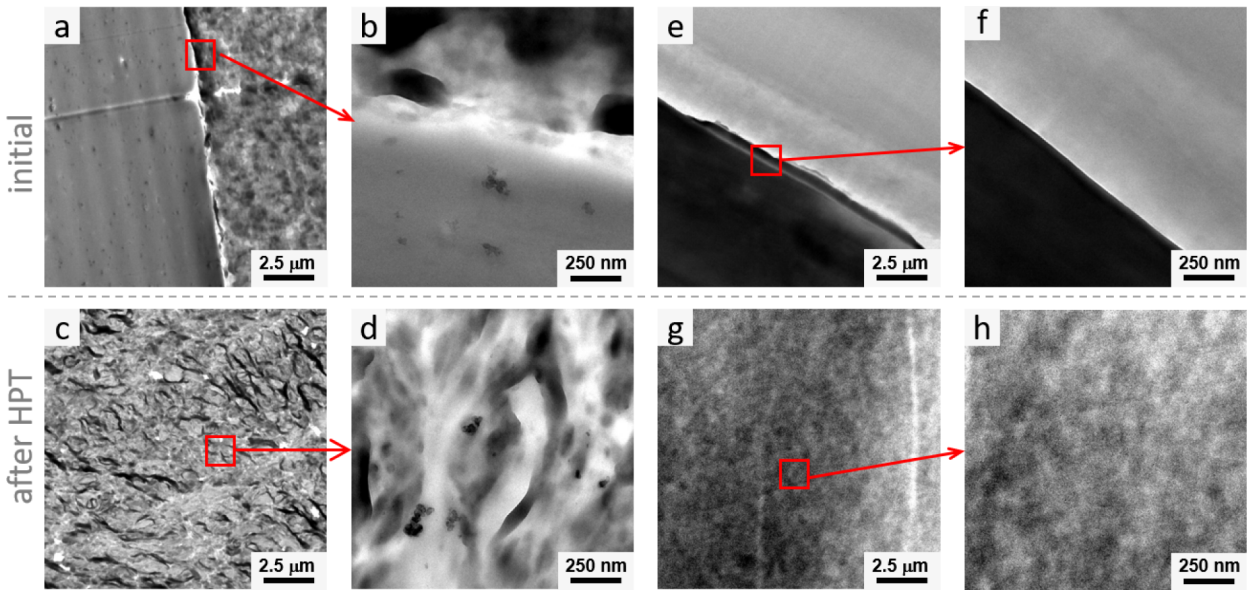

Figure 4. TEM images of ABS/PET (initial (a,b), HPT-processed (c,d)) and PET/PBT (initial (e,f), HPT-processed (g,h)) blends. Macroscopic phase-separated bilayer structures, where gray and pockmarked areas represent ABS and PET phases (a and b) and dark and bright areas correspond to PET and PBT phases (e and f), are observed in the images of initial ABS/PET and PET/PBT blends. In contrast, ABS/PET and PET/PBT blends processed using HPT show no clearly separated polymer phases (c,g). Even at high magnification (d,h), no obvious contrast is evident in the HPT-processed blends, suggesting the formation of a single phase or homogeneous mixing of ABS and PET, as well as PET and PBT in the blend samples.

protons in the blends. It should be noted, however, that a deviation from this rule is also possible if local concentration fluctuations occur in miscible blends, which can cause the occurrence of two glass transition temperatures in particular.[51−53]

Figure 2 shows the results of DSC and measurements of spin−lattice relaxation times of the investigated blends (acrylonitrile butadiene styrene copolymer/poly(ethylene terephthalate) (ABS/PET), polylactide/polybutylene terephthalate (PLA/PBT), polylactide/poly(ethylene terephthalate) (PLA/PET), poly(ethylene terephthalate)/polybutylene terephthalate (PET/PBT), high density polyethylene/polystyrene (HDPE/PS), and polypropylene/polystyrene (PP/PS) before and after HPT treatment.

It can be seen that the HPT treatment leads to a significant improvement in the degree of miscibility of the blended polymers. All polymer blends treated with HPT exhibit a single glass transition temperature that is typical for the case of a homogeneous mixing at the microscopic level of its constituent polymers. The T_1 values are quite close to each other. Although the difference between the spin−lattice relaxation times should tend toward zero, this value is several tenths of a second before the decimal point for true miscible polymer blends.[11,12,54] The resulting T_1 values indicate that the mixing of the polymers occurs at the range of tenths of a nanometer within the interphase. The closeness of the $T_{1\rho}$ values also indicates the homogeneity of the blends prepared with HPT on the nanometer scale. To approximate the upper limit of the mixing scale, the following one-dimensional diffusion equation can be used: $\langle L^2 \rangle = 6DT_i(H)$, where D is the spin diffusion coefficient that depends on both the average proton distance and the dipolar interaction. It has a typical value for polymeric systems of the order of $(4-6) \times 10^{-16}$ m^2 s^{-1}.[55] T_i is the relaxation time, $T_1(H)$ or $T_{1\rho}(H)$, according to the type of relaxation measurements. It is estimated that the polymers studied are intimately mixed on a scale of less than 20−40 nm.

Similar results were obtained for blends of already recycled counterparts (Figures 2c, 3). The efficiency of forming a homogeneous polymer blend based on thermodynamically incompatible polymers is not affected by at least 5 recycling cycles. The difference may consist of only slightly lower absolute values of glass transition and decomposition temperatures.

It is also noteworthy that mixing under HPT conditions was effective both for polymer pairs with relatively close solubility parameters δn ($\Delta\delta$n ≈ 0.4−1.0) such as PET/PBT, PLA/PBT, and PLA/PET and for polymer pairs with large difference between solubility parameters ($\Delta\delta$n ≈ 2.0) such as ABS/PET, HDPE/PS, and PP/PS.

To prove the miscibility of the studied polymers at the nanometer level, the nanoscale morphology of the polymer blends was analyzed by transmission electron microscopy (TEM). As an example, TEM images are shown for a system with relatively similar and significantly different solubility parameters: PET/PBT and ABS/PET, respectively. In the TEM images, the initial blends showed a macroscopically separated structure with the individual polymer layers, while the blends treated with HPT showed no obvious contrast on the nanometer scale (Figure 4), indicating that the mixing of the polymers occurs at the nanoscale. It is pertinent to note that at the micrometer level, nonprocessed blends exhibited a heterogeneous, two phase structure, while HPT-processed blends showed no discernible heterogeneity (Figure S2).

Morphology plays an important role and significantly influences the final properties of polymer blends. For a correct comparison of the mechanical properties of the HPT-processed blends, blends with the same content of components obtained by mixing in the melt with a Brabender-type mixer were prepared as initial blends. High-pressure solid-phase mixing of immiscible polymers is accompanied by a significant improvement in their performance. In fact, the microhardness of the HPT-treated blends increases by 15−30% compared to

https://doi.org/10.1021/acssuschemeng.4c04557
ACS Sustainable Chem. Eng. 2025, 13, 1203−1212

Table 1. Microhardness Values (H) and Dispersion of Microhardness (D_H) of Polymer Blends Before and After HPT Treatment

Blend	PET/PBT	PLA/PBT	PLA/PET	HDPE/PS	PP/PS	ABS/PET	r-HDPE/r-PS	r-PP/r-PS
H, MPa	87/114	98/120	78/95	48/54	57/65	75/93	35/40	43/49
D_H	5.82/0.45	4.52/0.43	3.06/0.50	6.50/0.77	5.30/0.64	2.07/0.35	6.24/1.05	5.91/0.97

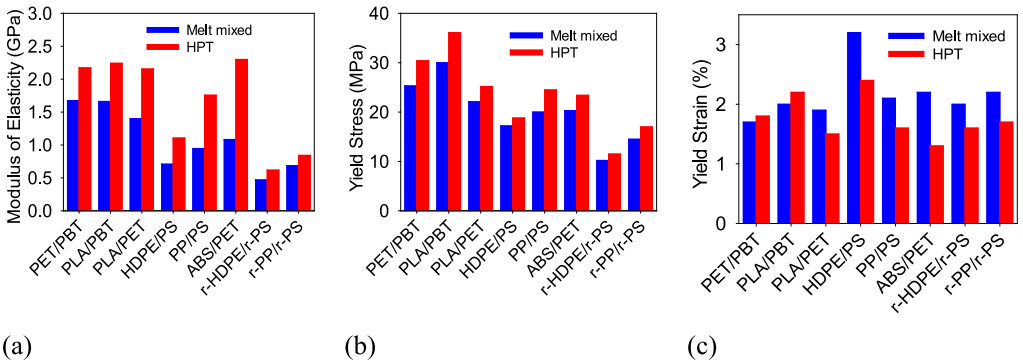

Figure 5. Diagrams showing the changes in the mechanical properties as a result of HPT treatment: (a) modulus of elasticity, (b) yield strength, and (c) yield strain of blends.

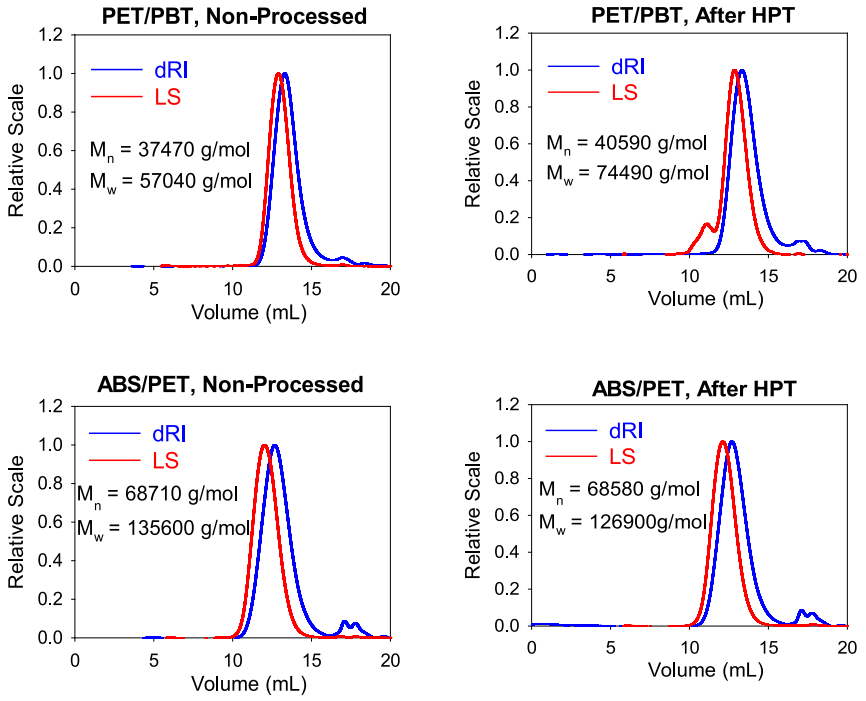

Figure 6. Light scattering (LS) and differential refractive index (dRI) chromatograms of PET/PBT and ABS/PET samples with measured molecular weights.

the initial blends (Table 1). It should be noted that the uniformity of the microhardness distribution on the surface of the samples changed drastically before and after HPT treatment (Table 1). All initial blends are characterized by a considerable dispersion of microhardness, which is due to a significant difference in the microhardness values of the corresponding polymer phases. In contrast, the HPT-treated blends are characterized by a low dispersion of microhardness. The latter indicates effective mixing of the polymer phases and the formation of a homogeneous structure.

In the numerator, the data for the initial blend are given. In the denominator, the data for the HPT-treated blend are given. To measure the microhardness of the initial blends, the components were mixed in the melt with a Brabender-type mixer. The microhardness of the original polymers is 90 MPa, 160 MPa, 98 MPa, 100 MPa, 32 MPa, 95 MPa, 50 MPa, 26 MPa, 80 MPa, and 43 MPa for PET, PBT, PLA, ABS, HDPE, PS, PP, r-HDPE, r-PS, and r-PP, respectively.

The results of the microhardness measurements correlate with the results of the uniaxial tensile test on melt mixed and the HPT-processed blends (Figure 5, Table S2). The representative stress−strain curves of the samples are shown in Figure S1. Compared to melt mixed blends, HPT-processed blends exhibit a 20−50% higher modulus of elasticity and a 10−20% higher yield strength. The increase in yield strength and elastic modulus of HPT-processed blends could be due to

https://doi.org/10.1021/acssuschemeng.4c04557
ACS Sustainable Chem. Eng. 2025, 13, 1203−1212

denser packing and increased interaction between the macromolecules of the polymer blend components in the interfacial contact region.[56,57] Although the plastic characteristics (Figure 5c) did not increase compared to the mixture obtained by using the Brabender mixer, they did not decrease either, which indirectly confirms that the application of high pressure during HPT leads to the complete healing of damage caused by enormous deformations.

When polymers are mixed under the influence of shear forces, mechanical destruction processes can occur that lead to the breakage of macromolecules with radicals forming at the breakage points. The resulting macroradicals can recombine at the interface between two immiscible polymers and thus increase the compatibility of the polymers in the mixture by reducing the interfacial tension and by mechanically blocking and "entangling" the macromolecules.[58−60] The results for the two systems ABS/PET and PET/PBT, which are characterized by high molecular weights (over 100 000) and medium molecular weights (over 50 000) show that HPT treatment leads to a slight decrease in weight-average M_w and number-average M_n molecular weights and polydispersity M_w/M_n (by 5−6%) for the first system and to an increase in molecular weights (M_n by 8%, M_w by 31%) for the second system, while polydispersity M_w/M_n is maintained (Figure 6). Thus, for HPT-treated high molecular weight blends, lower molecular weights can contribute to improving the compatibility of the polymers that compose them; for HPT-treated medium molecular weight blends (which can also be recycled polymers with high virgin molecular weight), higher molecular weights can contribute to improving or restoring the mechanical properties.

DISCUSSION

Proposed Mechanism for Solid Phase Mixing. A schematic representation of the polymer solid phase mixing mechanism proposed by the authors is shown in Figure 7. In

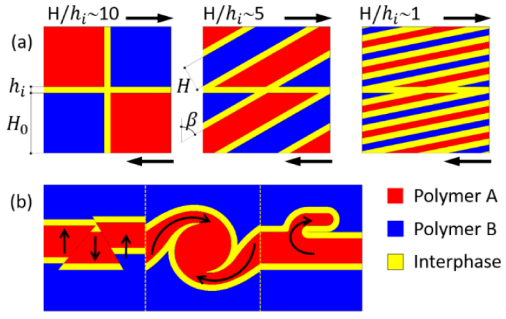

Figure 7. Schematic of the structural transformation in the polymer blend: (a) simple shear; (b) possible type of instabilities.

Figure 7a, a classic diagram illustrates material deformation by simple shear. The polymer components are color coded: red for polymer A, blue for polymer B, and yellow for the interphase—a region where partial mixing of even immiscible polymers occurs, with a thickness h_i in the order of several tens of nanometers. In the initial blends of polymers, the volume fraction of the interphase is insignificant, leading to a limited effect on polymer mixing. Under shear deformation $\gamma = \tan \beta$, the thickness H of the polymer blocks decreases while their length increases, what can be assessed as $H/H_0 = \cos \beta$. The higher the deformation, the thinner the layers of polymers A and B become. Although the thickness of interphase h_i remains constant, the increase in interface area leads to a higher volume fraction of the interphase. As the thickness of the polymer layers approaches that of the interphase $H/h_i \sim 1$, the blend transforms into a mixture composed entirely of the interphase. According to very rough estimates, a reduction in the thickness of the initial layers by approximately 1000 times can be achieved solely through a simple shear scheme with the number of anvil revolutions set at 50. This behavior is akin to a mixture of miscible polymers, characterized by a single glass transition temperature and a decomposition temperature. Figure 7b shows several possible manifestations of the instability effect—a phenomenon observed during shear deformation of an inhomogeneous medium.[61−63] This effect is characterized by the presence of random vertical components in the velocity field. Deviation from the ideal simple shear and the emergence of vertical velocity components can be linked to the presence of shear bands, the formation of folds, the occurrence of periodic vortices, or delamination. All these effects, both on the nano, micro, and macro scales, are also observed during HPT of metal layered workpieces. Identifying the nature of these effects is a fundamental task that extends beyond the scope of this work. However, it is crucial to note that when these instabilities are combined with simple shear, they result in a flow resembling turbulence, significantly enhancing the process of mechanical mixing.[40,61]

The successful application of solid-phase mixing of immiscible polymers necessitates adherence to two fundamental requirements: (i) The mixing temperature must remain below the glass transition temperatures or the melting temperatures of the polymers involved. This precaution prevents the undesirable process of interfacial tension, which can induce phase separation and impede the formation of a miscible, single-phase morphology. When deformation occurs in the solid phase without the polymer transitioning to a viscous state, it prevents the interfacial tension effect that leads to the decay of polymer layers into droplets, a phenomenon known as demixing. This characteristic enables a continuous reduction in the thickness of the polymer layers to match that of the interphase. Furthermore, it helps to prevent the undesirable degradation of lower melting components, a common issue in molten polymer blends processed at the temperature of the highest melting component. (ii) Plastic deformation must be extremely high and capable of mechanically reducing the thickness of the polymer phases to interphase sizes. This critical step transforms immiscible polymer blends into miscible blends, which was successfully met through the HPT method.

It is relevant to note that the long-term stability and performance of recycled materials are strongly influenced by the blend's miscibility. Immiscible blends tend to have phase separation, leading to the formation of weak interfaces and reducing overall mechanical, thermal oxidation, and ultraviolet stability. In contrast, miscible blends that form a uniform phase exhibit better stability. Fewer weak interfaces mean fewer regions where oxidative degradation can initiate. Our preliminary results on the determination of oxidation induction time (Figure S3) confirm that the blends processed with HPT, which are characterized by homogeneous mixing at the nanoscale, have 1.3−1.7 times higher oxidation induction time values than the nonprocessed immiscible blends. Further studies on the stability of HPT-processed blends, especially

https://doi.org/10.1021/acssuschemeng.4c04557
ACS Sustainable Chem. Eng. 2025, 13, 1203−1212

under different environmental conditions, will show their potential practical applicability. The results of 1H spin−lattice relaxation time measurements both in the laboratory and in rotating frames T_1 and $T_{1\rho}$ of samples stored at ambient conditions for 18 months (Table S3) give a positive prognosis for such studies. In particular, the relaxation times for the HPT-processed blends remained practically unchanged, which indicates the stability of the formed structure and the invariability of the length scale of homogeneity in polymer blends, which are still 20−40 nm. It can also be assumed that the HPT-processed blends may be more resistant to fragmentation and release of microplastics than the initial blends. Since the fragmentation rate is polymer-dependent,[64,65] immiscible blends are expected to undergo cascade fragmentation, starting with fragmentation in weak interphase layers and then fragmenting in individual polymer phases, which facilitates the effective formation of microplastics. At the same time, the presence of a uniform, homogeneously mixed phase and the absence of weak interphase layers in HPT-processed blends should lead to greater resistance to fragmentation and the release of microplastics. In the case of biobased and biodegradable blends, fragmentation can be accelerated by microorganisms. The absence of weak interphase layers, which are susceptible to microbial attack, should also have a positive effect on reducing the fragmentation rate and release of microplastics in HPT-processed blends. The prospects for recycling by solid-phase mixing are also that an immiscible ternary or multicomponent polymer system can be converted into miscible blends. In contrast, the compatibilization of such systems would be associated with the difficulty of producing an effective complex multiphase compatibilizer, as this is mainly used to compatibilize binary blends. Finally, note that the role of contamination in the efficiency of solid phase mixing remains to be investigated. However, it is known that some fillers, such as aerosil, asbestos, and acetyl black in quantities from 5 to 30 wt %, can promote efficient homogeneous mixing of polymers in the solid phase at lower pressures, while others, such as talc and titanium dioxide, have no significant effect on mixing efficiency.

In summary, we have successfully developed a completely new, environmentally friendly, safe, cost-effective, scalable, and efficient concept for recycling of bicomponent plastic waste. We utilized the mechanism of mechanical reduction of the thickness of polymer phases to nanosizes commensurate with the thickness of the interphase. In this way, the difference between polymer phases and interphases disappears, and the structure of the polymer mixture is achieved consisting entirely of the interphase. Technically, this can be achieved by using methods that allow for the continuous accumulation of plastic deformation in polymers without material failure, such as high-pressure torsion. The fundamental possibility of solid-phase mixing of immiscible polymers is demonstrated by the example of thermodynamically incompatible polymer pairs that make up the bulk of solid plastic waste, such as PET/PBT, PLA/PBT, PLA/PET, ABS/PET, HDPE/PS, and PP/PS and their recycling counterparts. Notably, high-pressure solid phase mixing is equally effective for polymer pairs with both similar solubility parameters and for those with extremely different solubility parameters.

The demonstrated approach has proven to be effective for homogenizing binary immiscible mixtures, offering optimistic prospects for the homogenization of ternary and multi-component immiscible mixtures, as well. The big challenge of industrial applications involves scaling up the technology. Nevertheless, the presented technology stands out for its innovation compared with existing approaches, and the results obtained affirm its promising potential for recycling plastic waste.

■ ASSOCIATED CONTENT

Supporting Information

The Supporting Information is available free of charge at https://pubs.acs.org/doi/10.1021/acssuschemeng.4c04557.

Figure S1A: Exemplary of the respective stress−strain dependencies determined during uniaxial tensile test on initial (nonprocessed) and HPT processed blends; Figure S1B: Stress−strain dependencies determined during uniaxial tensile test on initial (nonprocessed) and HPT processed blends; Figure S2: SEM images of PLA/PBT (initial (a), HPT-processed (b)) and PLA/PET (initial (c), HPT-processed (d)); Figure S3: Diagrams showing the changes in the mean oxidation induction time (OIT, minute) as a result of HPT treatment; Table S1: T_1 and $T_{1\rho}$ values of polymer blends before and after HPT treatment; Table S2: Modulus of elasticity and yield stress of blends before and after HPT treatment; Table S3: T1 and T1ρ values of polymer blends measured 18 months after HPT treatment (PDF)

■ AUTHOR INFORMATION

Corresponding Authors

Iurii Vozniak − *Centre of Molecular and Macromolecular Studies, Polish Academy of Sciences, Lodz 90-363, Poland*; orcid.org/0000-0002-8123-0689; Email: wozniak@cbmm.lodz.pl

Roman Kulagin − *Institute of Nanotechnology, Karlsruhe Institute of Technology, Eggenstein-Leopoldshafen 76344, Germany*; Email: roman.kulagin@kit.edu

Authors

Alina Vozniak − *Centre of Molecular and Macromolecular Studies, Polish Academy of Sciences, Lodz 90-363, Poland*

Ramin Hosseinnezhad − *Centre of Molecular and Macromolecular Studies, Polish Academy of Sciences, Lodz 90-363, Poland*

Artur Rozanski − *Centre of Molecular and Macromolecular Studies, Polish Academy of Sciences, Lodz 90-363, Poland*; orcid.org/0000-0001-7545-6246

Fahmi Zaïri − *Civil Engineering and geo-Environmental Laboratory (LGCgE), Lille University, Lille 59000, France*

Complete contact information is available at: https://pubs.acs.org/10.1021/acssuschemeng.4c04557

Author Contributions

‖All authors contributed equally.

Notes

The authors declare no competing financial interest.

■ ACKNOWLEDGMENTS

This research was funded in part by National Science Centre (Poland) under the grant 2021/43/B/ST8/01443 and Grant Nos. UMO-2021/43/B/ST8/01443 and UMO-2023/51/D/ST8/01325.

ABBREVIATIONS

HPT high-pressure torsion

REFERENCES

(1) World Economic Forum. *Ellen MacArthur Foundation and McKinsey & Company, New Plastics Economy: Rethinking The Future Of Plastics*. World Economic Forum, Switzerland, 2016.

(2) Lange, J.-P. Managing plastic waste - sorting, recycling, disposal, and product redesign. *ACS Sustainable Chem. Eng.* **2021**, *9*, 15722.

(3) Geyer, R.; Jambeck, J. R.; Law, K. L. Production, use, and fate of all plastics ever made. *Sci. Adv.* **2017**, *3*, No. e1700782.

(4) Ragaert, K.; Delva, L.; Van Geem, K. Mechanical and chemical recycling of solid plastic waste. *J. Waste Manag.* **2017**, *69*, 24.

(5) Hamad, K.; Kaseem, M.; Deri, F. Recycling of waste from polymer materials: An overview of the recent works. *Polym. Degrad. Stab.* **2013**, *98*, 2801.

(6) Rahimi, A.; García, J. M. Chemical recycling of waste plastics for new materials production. *Nat. Rev. Chem.* **2017**, *1*, 0046.

(7) Coates, G. W.; Getzler, Y. D. Y. L. Chemical recycling to monomer for an ideal, circular polymer economy. *Nat. Rev. Mater.* **2020**, *5*, 501.

(8) Yu, Y.; Fang, L.-M.; Liu, Y.; Lu, X.-B. Chemical synthesis of CO_2-based polymers with enhanced thermal stability and unexpected recyclability from biosourced monomers. *ACS Catal.* **2021**, *11*, 8349.

(9) Yang, R.; Xu, G.; Dong, B.; Guo, X.; Wang, Q. Selective, sequential, and "one-pot" depolymerization strategies for chemical recycling of commercial plastics and mixed plastics. *ACS Sustainable Chem. Eng.* **2022**, *10*, 9860.

(10) Qin, B.; Liu, S.; Huang, Z.; Zeng, L.; Xu, J.-F.; Zhang, X. Closed-loop chemical recycling of cross-linked polymeric materials based on reversible amidation chemistry. *Nat. Commun.* **2022**, *13*, 7595.

(11) Christensen, P. R.; Scheuermann, A. M.; Loeffler, K. E.; Helms, B. A. Closed-loop recycling of plastics enabled by dynamic covalent diketoenamine bonds. *Nat. Chem.* **2019**, *11*, 442.

(12) Lu, X.; Zhang, X.; Zhang, C.; Zhang, X. Cyclic polyesters with closed-loop recyclability from a new chemically reversible alternating copolymerization. *Adv. Sci.* **2024**, *11*, No. e2306072.

(13) Uekert, T.; Singh, A.; DesVeaux, J. S.; Ghosh, T.; Bhatt, A.; Yadav, G.; Afzal, S.; Walzberg, J.; Knauer, K. M.; Nicholson, S. R.; Beckham, G. T.; Carpenter, A. C. Technical, economic, and environmental comparison of closed-loop recycling technologies for common plastics. *ACS Sustainable Chem. Eng.* **2023**, *11*, 965.

(14) Häußler, M.; Eck, M.; Rothauer, D.; Mecking, S. Closed-loop recycling of polyethylene-like materials. *Nature* **2021**, *590*, 423.

(15) Zhang, X.; Guo, W.; Zhang, C.; Zhang, X. A recyclable polyester library from reversible alternating copolymerization of aldehyde and cyclic anhydride. *Nat. Commun.* **2023**, *14*, 5423.

(16) Mankar, S. V.; Wahlberg, J.; Warlin, N.; Valsange, N. G.; Rehnberg, N.; Lundmark, S.; Jannasch, P.; Zhang, B. Short-loop chemical recycling via telechelic polymers for biobased polyesters with spiroacetal units. *ACS Sustainable Chem. Eng.* **2023**, *11*, 5135.

(17) McGuire, T. M.; Deacy, A. C.; Buchard, A.; Williams, C. K. Solid-state chemical recycling of polycarbonates to epoxides and carbon dioxide using a heterodinuclear Mg(II) Co(II) catalyst. *J. Am. Chem. Soc.* **2022**, *144*, 18444−18449.

(18) Smith, M. L.; McGuire, T. M.; Buchard, A.; Williams, C. K. Evaluating heterodinuclear Mg(II)M(II) (M = Mn, Fe, Ni, Cu, and Zn) catalysts for the chemical recycling of poly(cyclohexene carbonate). *ACS Catal.* **2023**, *13*, 15770.

(19) Darensbourg, D. J.; Wei, S.-H.; Yeung, A. D.; Ellis, W. C. An efficient method of depolymerization of poly(cyclopentene carbonate) to its comonomers: cyclopentene oxide and carbon dioxide. *Macromolecules* **2013**, *46*, 5850.

(20) Yang, G.-W.; Wang, Y.; Qi, H.; Zhang, Y.-Y.; Zhu, X.-F.; Lu, C.; Yang, L.; Wu, G.-P. Highly selective preparation and depolymerization of chemically recyclable poly(cyclopentene carbonate) enabled by organoboron catalysts. *Angew. Chem., Int. Ed.* **2022**, *61*, No. e202210243.

(21) Wang, C.; Eisenreich, F.; Tomović, Ž. Closed-loop recyclable high-performance polyimine aerogels derived from bio-based resources. *Adv. Mater.* **2023**, *35* (8), 2209003.

(22) Qin, B.; Zhang, S.; Sun, P.; Tang, B.; Yin, Z.; Cao, X.; Chen, Q.; Xu, J.-F.; Zhang, X. Tough and multi-recyclable cross-linked supramolecular polyureas via incorporating noncovalent bonds into main-chains. *Adv. Mater.* **2020**, *32* (36), 2000096.

(23) Furgiuele, N.; Lebovitz, A. H.; Khait, K.; Torkelson, J. M. Novel strategy for polymer blend compatibilization: solid-state shear pulverization. *Macromolecules* **2000**, *33*, 225.

(24) Lebovitz, A. H.; Khait, K.; Torkelson, J. M. Stabilization of dispersed phase to static coarsening: Polymer blend compatibilization via solid-state shear pulverization. *Macromolecules* **2002**, *35* (23), 8672−8675.

(25) Maris, J.; Bourdon, S.; Brossard, J.-M.; Cauret, L.; Fontaine, L.; Montembault, V. Mechanical recycling: Compatibilization of mixed thermoplastic wastes. *Polym. Degrad. Stab.* **2018**, *147*, 245.

(26) Yang, X.; Song, J.; Wang, H.; Lin, Q.; Jin, X.; Yang, X.; Li, Y. Reactive comb polymer compatibilized immiscible PVDF/PLLA blends: effects of the main chain structure of compatibilizer. *Polymers* **2020**, *12*, 526.

(27) Will, T. A.; Lu, Y.; Wakabayashi, K. Effects of Polymer Properties on Solid-State Shear Pulverization: Thermoplastic Processability and Nanofiller Dispersibility. *ACS Appl. Polym. Mater.* **2023**, *5*, 1848.

(28) OECD. *Global Material Resources Outlook to 2060: Economic drivers and environmental consequences*; OECD, Paris, 2019.

(29) Lipatov, Y. Interphase phenomena in polymer blends. *J. Polym. Sci.* **1977**, *61*, 369.

(30) Park, T.; Zimmerman, S. C. Formation of a miscible supramolecular polymer blend through self-assembly mediated by a quadruply hydrogen-bonded heterocomplex. *J. Am. Chem. Soc.* **2006**, *128*, 11582.

(31) Sheiko, S. S.; Zhou, J.; Arnold, J.; Neugebauer, D.; Matyjaszewski, K.; Tsitsilianis, C.; Tsukruk, V. V.; Carrillo, J.-M. Y.; Dobrynin, A. V.; Rubinstein, M. Perfect mixing of immiscible macromolecules at fluid interfaces. *Nat. Mater.* **2013**, *12*, 735.

(32) Pan, C.; Sugiyasu, K.; Takeuchi, M. Blending conjugated polymers without phase separation for fluorescent colour tuning of polymeric materials through FRET. *Chem. Commun.* **2014**, *50*, 11814.

(33) Uemura, T.; Kaseda, T.; Sasaki, Y.; Inukai, M.; Toriyama, T.; Takahara, A.; Jinnai, H.; Kitagawa, S. Mixing of immiscible polymers using nanoporous coordination templates. *Nat. Commun.* **2015**, *6* (1), 7473.

(34) Clarke, R. W.; Sandmeier, T.; Franklin, K. A.; Reich, D.; Zhang, X.; Vengallur, N.; Patra, T. K.; Tannenbaum, R. J.; Adhikari, S.; Kumar, S. K.; Rovis, T.; Chen, E. Y.-X. Dynamic crosslinking compatibilizes immiscible mixed plastics. *Nature* **2023**, *616*, 731.

(35) Qu, J.; Huang, Z.; Yang, Z.; Zhang, G.; Yin, X.; Feng, Y.; He, H.; Jin, G.; Wu, T.; He, G.; Cao, X. Industrial-scale polypropylene−polyethylene physical alloying toward recycling. *Engineering* **2022**, *9*, 95−100.

(36) Zhang, S.-H.; Zhang, H.-H.; Liu, M.-J.; Liang, J.-F.; Deng, Y.-H.; Jiang, Y.-P.; Huang, Z.-X.; Qu, J.-P. Improving the anti-environmental stress cracking performance of amorphous polymer through volume pulsation injection molding with semi-crystalline polymer. *Polymer* **2024**, *308*, 127364.

(37) Liu, M.; Huang, Z.-X.; Xu, M.; Xu, J.; Zhang, S.; Zhao, Y.; Deng, G.; Qu, J.-P. Transparent intrinsic barrier polymer via dynamic pressure engineering. *Macromolecules* **2023**, *56*, 3585−3594.

(38) Huang, Y.-Z.; Liu, X.-X.; Huang, Z.-X.; Li, Y.-J.; He, H.-Z. From waste to wealth: upcycling waste polypropylene/polyethylene for thermal management via pressure-induced, flow-enhanced segregated structurizing with hexagonal boron nitride. *Ind. Eng. Chem. Res.* **2023**, *62*, 2710−2718.

https://doi.org/10.1021/acssuschemeng.4c04557
ACS Sustainable Chem. Eng. 2025, 13, 1203−1212

(39) Odunuga, S.; Li, Y.; Krasnochtchekov, P.; Bellon, P.; Averback, R. S. Forced chemical mixing in alloys driven by plastic deformation. *Phys. Rev. Lett.* **2005**, *95*, 045901.
(40) Pouryazdan, M.; Kaus, B. J. P.; Rack, A.; Ershov, A.; Hahn, H. Mixing instabilities during shearing of metals. *Nat. Commun.* **2017**, *8* (1), 1611.
(41) Kormout, K. S.; Pippan, R.; Bachmaier, A. Deformation-induced supersaturation in immiscible material systems during high-pressure torsion. *Adv. Eng. Mater.* **2017**, *19*, 1600675.
(42) Han, J.-K.; Herndon, T.; Jang, J.; Langdon, T. G.; Kawasaki, M. Synthesis of hybrid nanocrystalline alloys by mechanical bonding through high-pressure torsion. *Adv. Eng. Mater.* **2020**, *22* (4), 1901289.
(43) Beygelzimer, Y.; Estrin, Y.; Mazilkind, A.; Scherere, T.; Baretzky, B.; Hahn, H.; Kulagin, R. Quantifying solid-state mechanical mixing by high-pressure torsion. *J. Alloy. Compd.* **2021**, *878*, 160419.
(44) Lemonick, S. Chemical solutions for a chemical problem. *C&En Global Enterp.*; 2018, *96*, 25. .
(45) Kartalis, C. N.; Papaspyrides, C. D.; Pfaender, R. Recycling of post-used PE packaging film using the restabilizayion technique. *Polym. Degrad. Stab.* **2000**, *70*, 189−197.
(46) Waldman, W. R.; De Paoli, M. A. Thermo-mechanical degradation of polypropylene, low density polyethylene and their 1: 1 blend. *Polym. Degrad. Stab.* **1998**, *60*, 301.
(47) Remili, C.; Kaci, M.; Benhamida, A.; Bruzaud, S.; Grohens, Y. The effect of reprocessing cycles on the structure and properties of polystyrene/Cloisite 15A nanocomposites. *Polym. Degrad. Stab.* **2011**, *96*, 1489.
(48) Huang, J. M.; Yang, S. J. Studying the miscibility and thermal behavior of polybenzoxazine/poly(ε-caprolactone) blends using DSC, DMA, and solid-state 13C NMR spectroscopy. *Polymer* **2005**, *46*, 8068.
(49) Hosseinnezhad, R.; Vozniak, I.; Morawiec, J.; Galeski, A. Evolution of green in-situ generated polyamide nanofibers controlled by viscoelasticity. *Express Polym. Lett.* **2021**, *15*, 250−261.
(50) Olabisi, O.; Robeson, L. M.; Shaw, M. T. *Polymer-polymer miscibility*; Academic Press: New York, 1979.
(51) Lodge, T. P.; McLeish, T. C. B. Self-concentrations and effective glass transition temperatures in polymer blends. *Macromolecules* **2000**, *33*, 5278.
(52) Christie, D.; Register, R. A.; Priestley, R. D. Direct measurement of the local glass transition in self-assembled copolymers with nanometer resolution. *ACS Cent. Sci.* **2018**, *4* (4), 504−511.
(53) Pathak, J. A.; Colby, R. H.; Floudas, G.; Jerome, R. Dynamics in Miscible Blends of Polystyrene and Poly(vinyl methyl ether). *Macromolecules* **1999**, *32*, 2553.
(54) Kim, J.; Gray, M. K.; Zhou, H.; Nguyen, S. B. T.; Torkelson, J. M. Polymer blend compatibilization by gradient copolymer addition during melt processing: stabilization of dispersed phase to static coarsening. *Macromolecules* **2005**, *38*, 1037.
(55) Wang, J.; Cheung, M. K.; Mi, Y. Miscibility and morphology in crystalline/amorphous blends of poly(caprolactone)/poly(4-vinyl-phenol) as studied by DSC, FTIR, and 13C solid state NMR. *Polymer* **2002**, *43*, 1357.
(56) Erina, N. A.; Prut, E. V. Synergism of the elastic modulus of poly(propylene)-high-density poly(ethylene) blends. *Polym. Sci. A* **2000**, *42*, 183−188.
(57) Shklyaruka, B. F.; Gerasina, V. A.; Guseva, M. A.; Maletina, V. V. Influence of the Crystalline Structure of Components and the Boundary Layer between Them on Mechanical Properties of Polypropylene−High Density Polyethylene Composites. *Polym. Sci., Ser. A* **2021**, *63* (5), 533−541.
(58) Xanthos, M.; Dagli, S. S. Compatibilization of polymer blends by reactive processing. *Polym. Eng. Sci.* **1991**, *31*, 929.
(59) Janssen, L. P. B. M.; *Reactive extrusion systems*. Marcel Dekker, New York, 2004, pp. 246.
(60) Cavalieri, F.; Padella, F. Development of composite materials by mechanochemical treatment of post-consumer plastic waste. *J. Waste Manag.* **2002**, *22*, 913.
(61) Kulagin, R.; Beygelzimer, Y.; Ivanisenko, Y.; Mazilkin, A.; Straumal, B.; Hahn, H. Instabilities of interfaces between dissimilar metals induced by high pressure torsion. *Mater. Lett.* **2018**, *222*, 172.
(62) Sundaram, N. K.; Guo, Y.; Chandrasekar, S. Mesoscale folding, instability, and disruption of laminar flow in metal surfaces. *Phys. Rev. Lett.* **2012**, *109*, 106001.
(63) Gola, A.; Schwaiger, R.; Gumbsch, P.; Pastewka, L. Pattern formation during deformation of metallic nanolaminates. *Phys. Rev. Mater.* **2020**, *4*, 013603.
(64) Niu, Z.; Curto, M.; Le Gall, M.; Demeyer, E.; Asselman, J.; Janssen, C. R.; Dhakal, H. N.; Davies, P. R.; Catarino, A. I.; Everaert, G. Accelerated fragmentation of two thermoplastics (polylactic acid and polypropylene) into microplastics after UV radiation and seawater immersion. *Ecotoxicol. Environ. Saf.* **2024**, *271*, 115981.
(65) Song, Y. K.; Hong, S. H.; Jang, M.; Han, G. M.; Jung, S. W.; Shim, W. J. Combined effects of UV exposure duration and mechanical abrasion on microplastic fragmentation by polymer type. *Environ. Sci. Technol.* **2017**, *51*, 4368−4376.

https://doi.org/10.1021/acssuschemeng.4c04557
ACS Sustainable Chem. Eng. 2025, 13, 1203−1212